Identification of miR-15b as a transformation-related factor in mantle cell lymphoma

FUMIKO ARAKAWA[1], YOSHIZO KIMURA[1], NORIAKI YOSHIDA[1,2], HIROAKI MIYOSHI[1],
ATUSHI DOI[3], KAORI YASUDA[3], KAZUTAKA NAKAJIMA[1], JUNICHI KIYASU[1], DAISUKE NIINO[1],
YASUO SUGITA[1], KOSUKE TASHIRO[4], SATORU KUHARA[4], MASAO SETO[1,2] and KOICHI OHSHIMA[1]

[1]Department of Pathology, School of Medicine, Kurume University, Kurume; [2]Division of Molecular Medicine,
Aichi Cancer Research Institute, Nagoya; [3]Cell Innovator Inc., Venture Business Laboratory of
Kyushu University, Fukuoka; [4]Laboratory of Molecular Gene Technology and Molecular Biosciences,
Department of Bioscience and Biotechnology, Faculty of Agriculture, Kyushu University, Fukuoka, Japan

Abstract. Mantle cell lymphoma (MCL) is an aggressive B cell lymphoma with a poor prognosis. It is characterized by the t(11;14)(q13;q32) translocation, resulting in over-expression of CCND1. Morphologically, MCL is categorised into two types: classical MCL (cMCL) and aggressive MCL (aMCL), with a proportion of cMCL progressing to develop into aMCL. miRNAs are currently considered to be important regulators for cell behavior and are deregulated in many malignancies. Although several genetic alterations have been implicated in the transformation of cMCL to aMCL, the involvement of miRNAs in transformation is not known. In an effort to identify the miRNAs related to the transformation of MCL, miRNA microarray analyses were used for cMCL and aMCL cases. These analyses demonstrated significant differences in the expression of seven microRNAs based on a t-test (p-value <0.05); miR-15b was greatly upregulated in aMCL. Locked nucleic acid *in situ* hybridization showed increased staining of miR-15b in formalin-fixed paraffin-embedded sections of aMCL. These results correlated well with the microRNA microarray analysis. Although the molecular functions of miR-15b are largely unknown, it has been found to be associated with the cell cycle and apoptosis. However, the physiological significance of increased miR-15b in MCL is still unknown. Our present findings suggest that the upregulated expression of miR-15b is likely to play an important role in the transformation of cMCL to aMCL.

Correspondence to: Dr Fumiko Arakawa, Department of Pathology, School of Medicine, Kurume University, Asahi-machi 67, Kurume, Fukuoka, 830-0011, Japan
E-mail: arakawa_fumiko@med.kurume-u.ac.jp

Introduction

Mantle cell lymphoma (MCL) constitutes approximately 5% to 7% of all malignant lymphomas (1); a recent epidemiologic study reported that MCL has increased in the United States and Japan (2). MCL has a broad spectrum of clinicopathological characteristics with a variety of morphological forms; these include the indolent type, the morphological equivalent of classical MCL (cMCL), and a more blastoid and pleomorphic appearance representing the aggressive form of MCL (aMCL) (3). Many patients with MCL repeatedly relapse and gradually become resistant to treatment.

MCL is clinicopathologically characterized by the t(11;14)(q13;q32) translocation, resulting in CCND1 overexpression and SOX11 expression (3). These events are valuable for the diagnosis of MCL (4). MCL can exist without the *CCND1* translocation. More than half of such cases have been shown to possess *CCND2* translocation (5). Therefore, this strongly suggests that the molecular basis of MCL is cell cycle deregulation caused by translocation and subsequent overexpression of *CCND1* or *CCND2*. However, abnormal *CCND*-related gene expression is insufficient for the pathogenesis of MCL, and does not account for aggressiveness of MCL (3).

Unbiased and whole-genome analyses revealed that alteration of *CDKN2A*, *TP53*, *ATM*, and *NOTCH1* genes are related to MCL progression and the prognosis (3,6). The MCL international prognostic index (MIPI) with the Ki-67 proliferation index (7), and an index including information for TP53 and SOX11 have been shown to adequately reflect the clinical outcome of MCL (8). Our previous study revealed that MCL could be classified into three forms; classical, intermediate and aggressive types based on the pathological findings, and that the aggressive type had a significant poorer prognosis that the other types (9). We also compared gene expression profiles of cMCL and aMCL and found that cell cycle regulation genes such as *CDK1*, *BIRC5*, and *FOXM1* are involved in transformation of cMCL to aMCL (10).

Through recent technical innovations, miRNAs, that are non-coding RNAs approximately 18-25 nucleotides in length, have been found to regulate gene expression. It is known that

multiple genes can be regulated by a single miRNA, and therefore, abnormal miRNA expression can deregulate expression of a number of genes. In fact, it has been reported that for some malignancies, including MCL, pathophysiological tumor status is closely associated with miRNA expression (11,12). miRNAs are also valuable for the diagnosis of some types of malignancies (13). In previous studies, high miR-17-92 expression in MCL was found to be associated with the transformation (14); low miR-34a expression correlates with the prognosis of MCL (15). However, miRNAs related to the progression of MCL remain to be delineated.

In this study, we used a 3D-Gene miRNA microarray and locked nucleic acid (LNA) *in situ* hybridization in formalin-fixed paraffin-embedded (FFPE) sections to identify miRNAs whose expression correlates with progression from cMCL to aMCL.

Materials and methods

Patients and tissue samples. We performed miRNA microarray experiments using frozen tissues from nine MCL lymph node specimens collected from the Department of Pathology of Kurume University (Fukuoka, Japan) (Table I). MCL was diagnosed according to the World Health Organization (WHO). MCL samples analyzed in this study, all of which were included in authors' previous study (10), are confirmed to carry the chromosomal translocation t(11;14)(q13;q32) (IgH/CCND1) and expression of CCND1 and SOX11 proteins. Categorization of MCL in this study were done based on WHO classification. The details are declared in the previous study (9). Briefly, 'Classical type' has morphological characteristics of classical MCL in WHO classification. 'Aggressive type' includes morphological features of blastic variant or pleomorphic variant of MCL in WHO classification. 'Intermediate type' has morphological transition in one section from region classified in classical type to region done in aggressive type. Of all 9 MCL specimens, 4 specimens were categorized in classical type (cMCL), 4 specimens were aggressive type (aMCL), and 1 specimen was intermediate type (iMCL, n=1). For iMCL, the region of classical MCL (iMCL-c, n=1) and the region of aggressive MCL (iMCL-a, n=1) were obtained by laser microdissection (LMD). This study was approved by the Kurume University Institutional Review Board and in accordance with the Declaration of Helsinki. Informed consent was not obtained because the data were analyzed anonymously.

Laser microdissection (LMD). The tissue samples were immediately frozen in acetone/dry ice and stored at -80˚C for microdissection. The iMCL sample was embedded in an optical cutting temperature (OCT) compound (Sakura Finetek, Tokyo, Japan) and frozen in liquid nitrogen. Cryosections (20 μm-thick) were mounted on 2.0 μm-thick PEN-Membrane slides (MicroDissect GmbH, Herborn, Germany). After fixation in 100% ethanol, the slides were stained rapidly with toluidine blue O (Chroma-Gesellschaft Schmid GmbH & Co., Köngen, Germany), washed with diethylpyrocarbonate (DEPC)-treated water, and air-dried using a fan.

The frozen sections were microdissected with a Leica LMD6000 laser microdissection system following the manufacturer's protocol (Leica, Wetzlar, Germany). The classical or aggressive parts were microdissected from the same iMCL tissue sections with LMD. The dissected cells were collected in 0.5-ml tube caps filled with 50 μl lysis buffer for RNA extraction (10,16).

RNA extraction and 3D-Gene miRNA expression microarray. Total RNA was isolated from frozen whole tumor tissue samples (cMCL and aMCL) with TRIzol (Invitrogen, Carlsbad, CA, USA). For the laser-dissected samples (iMCL-c and iMCL-a), total RNA was extracted with an RNAqueous-Micro kit (Ambion, Austin, TX, USA) according to the manufacturer's instructions for LMD. RNA samples were quantified with an ND-1000 spectrophotometer (NanoDrop Technologies, Wilmington, DE, USA) and the quality was confirmed with an Experion System (Bio-Rad Laboratories, Hercules, CA, USA).

miRNA expression profiling. Extracted total RNA was labeled with Hy5 using the miRCURY LNA™ microRNA Hy5 Power labelling kit (Exiqon, Vedbaek, Denmark). Labeled RNAs were hybridized onto 3D-Gene Human miRNA Oligo chips (v.14 1.0.1; Toray Industries, Tokyo, Japan). The annotation and oligonucleotide sequences of the probes were confirmed in the miRBase miRNA database Release 14 (http://microrna. sanger.ac.uk/sequences/). After stringent washes, fluorescent signals were scanned with the ScanArray Lite Scanner (Perkin Elmer, Waltham, MA, USA) and analyzed with GenePix Pro software (Molecular Devices, Sunnyvale, CA, USA).

Data processing. Raw data were normalized by subtracting the mean intensity of the background signal, as determined from the signal intensities of all blank spots, with 95% confidence intervals. Signal intensities >2 standard deviations (SD) of the background signal intensity were considered to be valid. Relative expression of a given miRNA was calculated by comparing the signal intensities of the averaged valid spots with their mean value throughout the microarray experiments.

Statistical analysis of microarray. The data were normalized, and the significantly differentially expressed miRNAs were obtained by comparing cMCL with aMCL using a t-test (p-value <0.05). A heat map of expression data from the selected miRNAs was generated with MeV software (www. tm4.org) (17). Ingenuity Pathway Analysis (IPA6.0; Ingenuity Systems, Redwood, CA, USA; www.ingenuity.com) was used to identify miRNA interaction with genes.

LNA in situ hybridization. Locked nucleic acid (LNA)-modified probes labeled with DIG (mercury-LNA detection probe) were obtained from Exiqon. The probe sequences were as follows: miR-15b, 5'-TGTAAACCATGATGTGCTGCTA-3' (5'-DIG and 3'-DIG); Scramble-miR used for negative control, 5'-GTGTAACACGTCTATACGCCCA-3' (5'-DIG); and U6 snRNA for positive control, 5'-CACGAATTTGCGTG TCATCCTT-3' (5'-DIG). FFPE tissues section, 6-μm thin adhered to glass slides were deparaffinized in two consecutive xylene baths for 15 min each, followed by 5 min each in serial dilutions of ethanol (100, 95 and 70%) and were washed with PBS. Slides were then digested with Histo/Zyme (Diagnostic

Table I. Clinical data of mantle cell lymphoma (MCL) used for miRNA microarray analysis.

Case no. (sample no.)	Age (year)	Gender	Diagnosis	Tissue	Growth pattern[d]	Ki-67 (%)	Translocation t(11;14)	RNA extraction
126	79	M	cMCL[a]	LN	N	25	+	Whole
135	59	M	cMCL	LN	N	20	+	Whole
141	75	M	cMCL	LN	N	25	+	Whole
200	75	M	cMCL	LN	N	30	+	Whole
5	71	M	aMCL[b]	LN	D	70	+	Whole
98	87	M	aMCL	LN	D	95	+	Whole
102	77	M	aMCL	LN	D	75	+	Whole
107	76	M	aMCL	LN	D	60	+	Whole
132	67	F	iMCL[c]	LN	N & D	15/95	+	
(132-C)			Classical part			15		LMD[e]
(132-A)			Aggressive part			95		LMD

[a]cMCL, classical MCL; [b]aMCL, aggressive MCL; [c]iMCL, intermediate MCL; [d]Growth pattern was evaluated for either nodular (N) or diffuse (D). [e]LDM, laser microdissection.

Biosystems, Pleasanton, CA, USA) at room temperature for 10 min, washed twice with PBS, fixed with 4% paraformaldehyde, and rinsed in PBS. For the hybridization step, the IsHyb In Situ Hybridization (ISH) kit (Biochain Institute Inc., Hayward, CA, USA) was used according to the manufacturer's instructions. Briefly, DIG-labeled LNA probes were denatured by heating to 90˚C for 4 min and diluted to 10-100 nM in the IsHyb kit hybridization solution. Slides were hybridized overnight at 50˚C in a Dako hybridizer (Dako, Glostrup, Denmark). After hybridization, slides were washed in pre-heated saline-sodium citrate (SSC) buffers at 50˚C: in 2X SSC for 10 min, 1X SSC for 10 min, and 0.2X SSC for 5 min. Then, slides were placed in 0.2X SSC at 37˚C for 10 min. Slides were incubated in 1x IsHyb kit blocking solution for 60 min at room temperature. Alkaline phosphatase (AP)-conjugated anti-DIG from the IsHyb kit was diluted 1:100 in PBS and applied to slides for 3 h at room temperature, followed by three washes in PBS. After two 5-min washes with 1X AP buffer, slides were incubated with nitro-blue tetrazolium chloride/5-Bromo-4-Chloro-3'-Indolylphosphatase p-Toluidine salt (NBT/BCIP) solution from the IsHyb kit, in the dark, overnight at room temperature to develop the dark-blue NBT-formazan precipitate. Images were converted to grayscale and analyzed using the image processing and analysis software Multi Gauge ver. 3.0 (FujiFilm, Tokyo, Japan). Formalin-fixed paraffin-embedded MCL tissue samples (n=31; 19 cMCL, 3 iMCL and 9 aMCL) and non-tumorous lymph node (LN) (n=8) were analyzed.

Immunohistochemistry and microscopic analysis. The MCL FFPE sections (19 cMCL, 3 iMCL and 9 aMCL) used for *in situ* hybridization were stained with haematoxylin-eosin. The immunohistochemical staining of MIB1 (Ki-67: DakoCytomation, Glostrup, Denmark) was performed. Expression was scored on a four-point scale as follows: grade 0, 0-10% of the tumor cells stained; grade 1, 10-40% stained; grade 2, 40-70% stained; grade 3, >70% stained.

Clinical and pathological findings for different groups were compared using the Student's t-test and the χ^2 test. Values were considered significant at $p<0.05$. The immunohistochemical analyses of p53 (mouse MAb clone DO-7: Dako Cytomation, Glostrup, Denmark) and c-myc (rabbit MAb clone Y69: Abcam, Cambridge, UK) were carried out.

Results

miRNA microarray: selection of candidate miRNA. We performed global miRNA expression analysis for cMCL (n=5) and aMCL (n=5) using the 3D-Gene Human miRNA Oligo chip (v.14 1.0.1; Toray) (Table I). The results showed that 7 microRNAs are significantly differentially expressed (Fig. 1 and Table III, p<0.05, t-test) between these two MCL forms. Comparing aMCL to cMCL it was observed that miR-130b, miR-15b, and miR-107 were significantly upregulated, while miR-92a-1*, miR-509-5p, miR-519e*, and miR-562 were downregulated (Table III).

Among the miRNAs identified by these miRNA microarray analyses, we focused on a miRNA which had fold change of >2 with mean signal intensity of >100. Only miR-15b (FC: 2.37, Mean signal intensity; cMCL: 292, aMCL: 690.8) fitted these criteria. This analysis raises the possibility that miR-15b plays an important role in the aggressive transformation from cMCL to aMCL.

LNA in situ hybridization: validation of miR-15b expression. To validate the results of global miRNA microarray analysis, we performed *in situ* hybridization using a mercury-LNA detection probe (Exiqon) to assess miR-15b expression. *In situ* hybridization was carried out for MCL Case 132, the intermediate MCL (iMCL) used for miRNA array analysis. Additionally, cMCL (19 cases), aMCL (8 cases), iMCL (3 cases), and reactive LN (8 cases) samples were also analyzed (Table II). Staining intensity of miR-15b was evaluated using
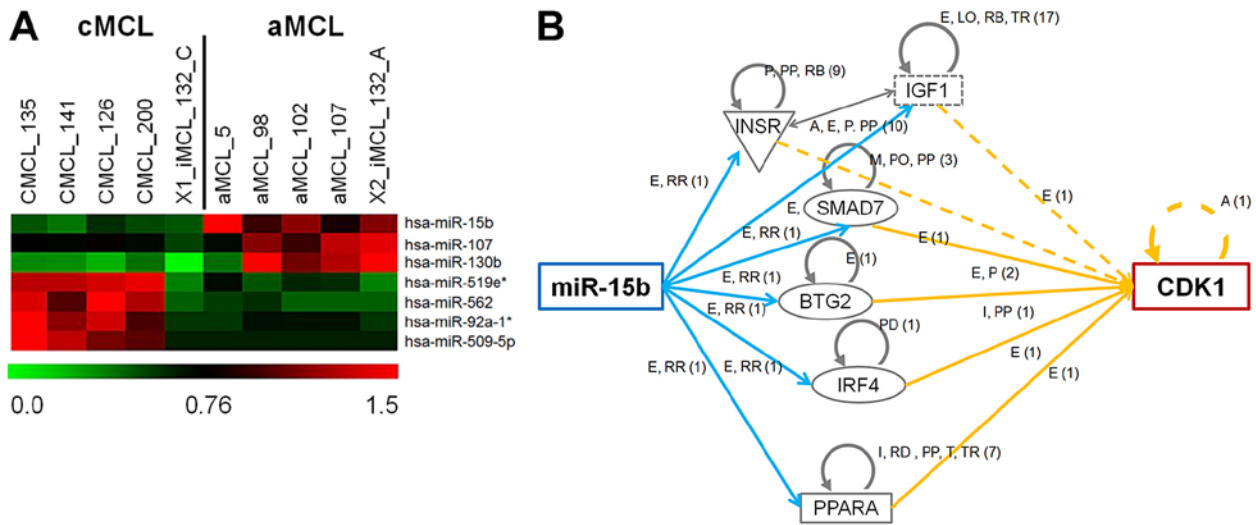
Figure 1. miRNA expression profile of MCL. (A) Heat map analysis of miRNA microarray data shows seven miRNAs whose expression levels are significantly different between aggressive MCL (aMCL) and classical MCL (cMCL) (p-value <0.05, t-test). Color intensity represents the magnitude of deviation from the median. Red represents high expression levels and green represents low expression levels. Among these miRNAs, miR-15b shows fold change of >2 with mean signal intensity of >100. (B) Gene network generated through the use of ingenuity pathways analysis (IPA). The relationship network between miR-15b and CDK1, which was observed to be upregulated in our previous cDNA expression array, was investigated by IPA. Although the chart showed an indirect relationship between miR-15b and CDK1, the genes are related to each other.

image analysis software (Multi Gauge version 3.0). Fig. 2A shows a representative example of miR-15b staining for iMCL (MCL Case 132). This case exhibits morphological features of both classical and aggressive forms in the same tissue. Comparison of the two morphological forms, miR-15b intensity in the aggressive form was 2.1-fold higher than in the classical form (Fig. 1A), which correlated well with the result of miRNA array analysis (2.32-fold change, Table III). This finding suggests that miR-15b expression is significantly important in aggressive MCL.

Of note, in the reactive lymph node, miR-15b expression was higher in the germinal center; only very few cells of the mantle zone, the cells affected by MCL, expressed miR-15b (Fig. 2B).

Correlation of miR-15b expression and MIB-1-positive cells. MIB-1 labeling index correlates with the aggressiveness of MCL, and is included in MIPI. Therefore, we evaluated a correlation between miR-15b expression and MIB-1 index. The result indicated a significant positive correlation between the two (ϱ=1.1005, R2=0.6287) (Fig. 3). No correlations were seen with p53 or c-myc.

In our previous study, gene expression analysis comparing cMCL and aMCL demonstrated that CDK1 expression was associated with a shift from cMCL to aMCL (10). In addition, ingenuity pathway analysis demonstrated that a connection between expression of CDK1 and miR-15b exists (Fig. 1B). These results suggest that miR-15b expression is more important in aMCL than cMCL.

Discussion

We have evaluated miRNA expression between cMCL and aMCL and found that high expression of miRNA-15b is characteristic of aMCL relative to cMCL. In our previous study, we

analyzed to the relationship between morphological subtypes of MCL and prognostic factors statistically. aMCL had the strongest Ki-67 positivity and showed extremely poor prognosis (9). miR-15b expression correlated with Ki-67, indicating that aMCL show high level expression (Fig. 3A). miR-15 expression is likely to be involved in progression of MCL.

Previous studies on miRNAs in MCL compared MCL cells with normal B cells or were evaluated using unsupervised hierarchical clustering (11,14). In the present study, we focused on the clinicopathological subtypes of MCL, aMCL and cMCL, and studied miRNA expression. We identified miR-15b as a novel miRNA, that is highly expressed in aMCL. Similar analysis was conducted for chronic lymphocytic lymphoma (CLL), but miR-15 was not identified (17). We further demonstrated that high expression of miR-15b is associated with aggressiveness using aMCL and cMCL samples from the same case (MCL Case 132) (Fig. 2A).

miR-15b is located at chromosome 3q25.33. Several genomic analyses including our previous study showed that gain of chromosome 3q, including the *MIR15B* locus, is frequently observed in MCL, even in the cMCL form (19,20). These findings indicated that high expression of miR-15b might be driven by mechanisms other than genomic copy number change. LNA *in situ* hybridization identified that high expression of miR-15b was found in germinal center cells but not in cells in the mantle zone, the normal cellular counterpart of MCL. This may simply reflect cell proliferation occurring in germinal center cells. Alternatively, this may reflect DNA damage and repair in germinal center cells, because miR-15b expression is reported to be induced either by radiation, hydrogen peroxide, or etoposide in human fibroblasts (21). miR-15b targets CCND3, CCNE1 and CDK6. It regulates the cell cycle (22) and is also involved in TP53 phosphorylation through ATM and CHK1 (23). From these findings, we speculate that expression of miR-15b is upregulated by DNA damage and repair.
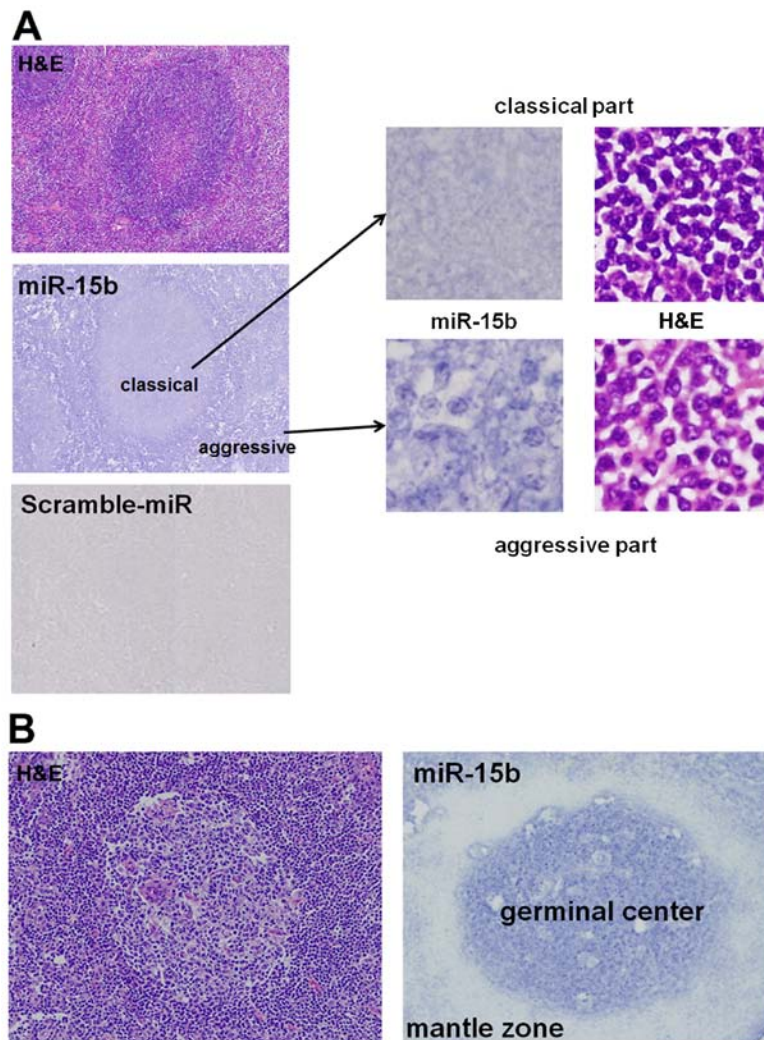
Figure 2. MCL *in situ* hybridization using miR-15b LNA probe. (A) miR-15b *in situ* hybridization pattern in a representative case (MCL Case 132). This sample shows both classical form (cMCL) and aggressive form (aMCL) in the same tissue section. Right upper panel shows the cMCL part and right lower panel shows the aMCL part. The miR-15b intensity in the aMCL is 2.1-fold higher than the intensity in cMCL. H&E, hematoxylin and eosin staining; miR-15b, miR-15 *in situ* hybridization, NBT/BCIP coloring (probe 100 nM); Scramble-miR, negative control (probe 10 nM) (x100). (B) miR-15b *in situ* hybridization for reactive lymph node (control LN) (x200). In control LN, miR-15b was highly expressed in germinal center cells and stained minimally in mantle zone cells, the normal cellular counterpart to MCL.
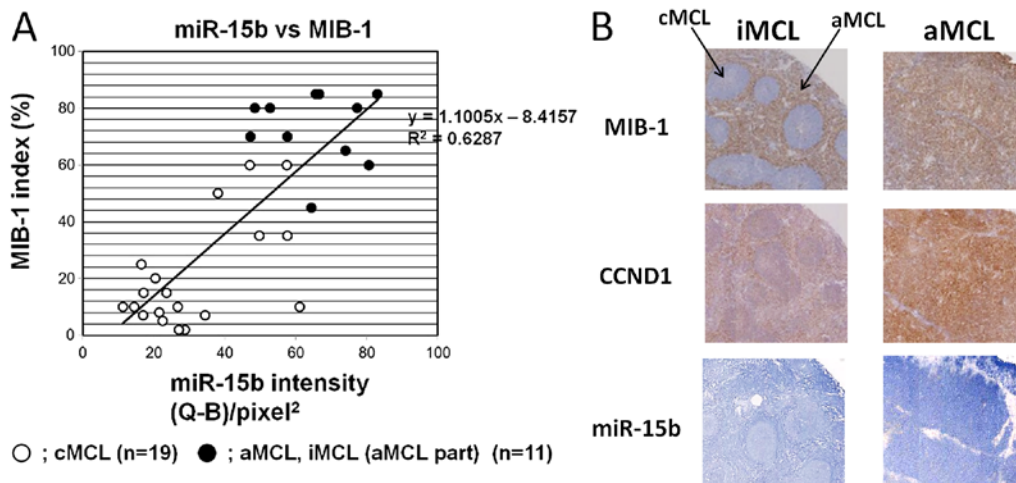

Figure 3. Relationship between miRNA-15b and MIB-1 expression in MCL. (A) The correlation of miR-15b expression by *in situ* hybridization and MIB-1 protein expression by immunostaining was analyzed. Expression of miR-15b and MIB-1 are higher in aMCL (n=11) than in cMCL (n=19). miR-15b and MIB-1 expression are significantly positively correlated ($p_{(rko)}$=1.1005, R2=0.6287). (B) Immunohistochemical staining of MIB-1 and CCND1, and miR-15b *in situ* hybridization staining of MCL. Immunohistochemical analysis indicated strong expression of MIB-1 and CCND1 at the protein level in aMCL. miR-15b *in situ* hybridization staining was strong in aMCL (x40).

Table II. Characteristics of MCL cases analyzed in the current study.

Case no.	Diagnosis	PI (Ki-67)	miR-15b intensity (Q-B)/pixel^2	miRNA microarray	LNA *in situ* hybridization
126	Classical (cMCL)	25		●	
135	cMCL	15	23.69	●	●
141	cMCL	10	61.07	●	●
200	cMCL	30		●	
5	Aggressive (aMCL)	70		●	
98	aMCL	95		●	
102	aMCL	75		●	
107	aMCL	60		●	
132	Intermediate (iMCL)	15/95			
(132-C)	Classical part	15	-	●	●
(132-A)	Aggressive part	95	-	●	●
1-A1	cMCL	10	11.37		●
1-A2	cMCL	7	34.52		●
1-A3	cMCL	8	21.69		●
1-A6	cMCL	20	20.48		●
1-B1	cMCL	60	47.1		●
1-B3	cMCL	7	17.02		●
1-B4	cMCL	2	28.83		●
1-B6	cMCL	25	16.51		●
1-C2	cMCL	35	49.84		●
1-C3	cMCL	15	17.26		●
1-C4	cMCL	10	26.85		●
1-C5	cMCL	50	38.09		●
1-C6	cMCL	5	22.6		●
1-D1	cMCL	60	57.5		●
1-D2	cMCL	35	57.61		●
1-D4	cMCL	10	14.59		●
1-D5	cMCL	2	27.09		●
2-A1	iMCL	60	80.63		●
2-A2	iMCL	80	77.33		●
2-A3	iMCL	80	48.51		●
2-A4	aMCL	85	65.68		●
2-A6	aMCL	70	47.25		●
2-B1	aMCL	45	64.36		●
2-B2	aMCL	85	83.03		●
2-B3	aMCL	70	57.71		●
2-B4	aMCL	65	74.07		●
2-B5	aMCL	80	52.77		●
2-B6	aMCL	85	66.57		●

The biological role of miR-15b in tumors is controversial. miR-15b is reported to be upregulated in squamous cell carcinoma of the head and neck (24), while the expression is decreased in progressed, aggressive gliomas (25). Unbiased and whole-genome analyses revealed that in MCL, CCND1 is deregulated, with genomic aberrations of *TP53, CDKN2A, RB1*, and *ATM*, suggesting that the DNA damage response is profoundly targeted (3). miR-15b is thought to be a negative regulator for CCND1 (24), but most MCL samples exhibit CCND1 protein expression. This may indicate a loss of the suppressive effect of miR-15 for CCND1 in MCL. Thus, miR-15b expression does not play a role as a negative regulator of the cell cycle in MCL, but instead plays a role in the pathophysiology of aMCL through different pathways.

Table III. List of up- and down-regulated miRNAs in MCL (aMCL versus cMCL).

miRNA	Chromosomal locus	Mean signal intensity		Fold change (FC) (aMCL/cMCL)	Log$_2$ FC	P-value
		cMCL	aMCL			
Upregulated						
hsa-miR-130b	22q11.21	10.3	45.4	4.41	2.14	0.016
hsa-miR-15b	3q25.33	292.0	690.8	2.37	1.24	0.018
hsa-miR-107	10q23.31	468.6	730.3	1.56	0.64	0.038
Downregulated						
hsa-miR-92a-1*	13q31.3	1.9	1.1	0.58	-0.78	0.045
hsa-miR-509-5p	Xq27.3	1.7	1.0	0.57	-0.80	0.033
hsa-miR-519e*	19q13.42	3.0	1.5	0.49	-1.02	0.045
hsa-miR-562	2q37.1	2.5	1.1	0.44	-1.20	0.036

Recently, Lovat et al [26] declared that the low expression of the miR-15b is important in B-cell lymphoma, in particular in the pathogenesis of CLL. In terms of transformation of MCL, high expression of miR-15b is speculated to be involved. At that case, targets of miR-15b is likely to be the other genes other than CCND1. CDK1 will be considered as one of its target genes.

In summary, we found that miR-15b is highly expressed in aMCL, is correlated with Ki-67 expression, and corresponds well with cancer aggressiveness. The relationship between high expression of miR-15b and MCL aggressiveness may potentially lead to new MCL therapy targets, but will require further study.

Acknowledgements

References

1. Goy A and Kahl B: Mantle cell lymphoma: The promise of new treatment options. Crit Rev Oncol Hematol 80: 69-86, 2011.
2. Chihara D, Ito H, Matsuda T, Shibata A, Katsumi A, Nakamura S, Tomotaka S, Morton LM, Weisenburger DD and Matsuo K: Differences in incidence and trends of haematological malignancies in Japan and the United States. Br J Haematol 164: 536-545, 2014.
3. Jares P, Colomer D and Campo E: Molecular pathogenesis of mantle cell lymphoma. J Clin Invest 122: 3416-3423, 2012.
4. Mozos A, Royo C, Hartmann E, De Jong D, Baró C, Valera A, Fu K, Weisenburger DD, Delabie J, Chuang SS, et al: SOX11 expression is highly specific for mantle cell lymphoma and identifies the cyclin D1-negative subtype. Haematologica 94: 1555-1562, 2009.
5. Salaverria I, Royo C, Carvajal-Cuenca A, Clot G, Navarro A, Valera A, Song JY, Woroniecka R, Rymkiewicz G, Klapper W, et al: CCND2 rearrangements are the most frequent genetic events in cyclin D1(-) mantle cell lymphoma. Blood 121: 1394-1402, 2013.
6. Kridel R, Meissner B, Rogic S, Boyle M, Telenius A, Woolcock B, Gunawardana J, Jenkins C, Cochrane C, Ben-Neriah S, et al: Whole transcriptome sequencing reveals recurrent NOTCH1 mutations in mantle cell lymphoma. Blood 119: 1963-1971, 2012.
7. Hoster E, Dreyling M, Klapper W, Gisselbrecht C, van Hoof A, Kluin-Nelemans HC, Pfreundschuh M, Reiser M, Metzner B, Einsele H, et al; German Low Grade Lymphoma Study Group (GLSG): European Mantle Cell Lymphoma Network: A small prognostic index (MIPI) for patients with advanced-stage mantle cell lymphoma. Blood 111: 558-565, 2008.
8. Nordström L, Sernbo S, Eden P, Grønbaek K, Kolstad A, Räty R, Karjalainen ML, Geisler C, Ralfkiaer E, Sundström C, et al: SOX11 and TP53 add prognostic information to MIPI in a homogenously treated cohort of mantle cell lymphoma - a Nordic Lymphoma Group study. Br J Haematol 166: 98-108, 2014.
9. Kimura Y, Sato K, Arakawa F, Karube K, Nomura Y, Shimizu K, Aoki R, Hashikawa K, Yoshida S, Kiyasu J, et al: Mantle cell lymphoma shows three morphological evolutions of classical, intermediate, and aggressive forms, which occur in parallel with increased labeling index of cyclin D1 and Ki-67. Cancer Sci 101: 806-814, 2010.
10. Kimura Y, Arakawa F, Kiyasu J, Miyoshi H, Yoshida M, Ichikawa A, Niino D, Sugita Y, Okamura T, Doi A, et al: The Wnt signaling pathway and mitotic regulators in the initiation and evolution of mantle cell lymphoma: Gene expression analysis. Int J Oncol 43: 457-468, 2013.
11. Teshima K, Nara M, Watanabe A, Ito M, Ikeda S, Hatano Y, Oshima K, Seto M, Sawada K and Tagawa H: Dysregulation of BMI1 and microRNA-16 collaborate to enhance an anti-apoptotic potential in the side population of refractory mantle cell lymphoma. Oncogene 33: 2191-2203, 2014.
12. Yamagishi M, Nakano K, Miyake A, Yamochi T, Kagami Y, Tsutsumi A, Matsuda Y, Sato-Otsubo A, Muto S, Utsunomiya A, et al: Polycomb-mediated loss of miR-31 activates NIK-dependent NF-κB pathway in adult T cell leukemia and other cancers. Cancer Cell 21: 121-135, 2012.
13. Liu AM, Yao TJ, Wang W, Wong KF, Lee NP, Fan ST, Poon RT, Gao C and Luk JM: Circulating miR-15b and miR-130b in serum as potential markers for detecting hepatocellular carcinoma: A retrospective cohort study. BMJ Open 2: e000825, 2012.
14. Iqbal J, Shen Y, Liu Y, Fu K, Jaffe ES, Liu C, Liu Z, Lachel CM, Deffenbacher K, Greiner TC, et al: Genome-wide miRNA profiling of mantle cell lymphoma reveals a distinct subgroup with poor prognosis. Blood 119: 4939-4948, 2012.
15. Navarro A, Clot G, Prieto M, Royo C, Vegliante MC, Amador V, Hartmann E, Salaverria I, Beà S, Martín-Subero JI, et al: microRNA expression profiles identify subtypes of mantle cell lymphoma with different clinicobiological characteristics. Clin Cancer Res 19: 3121-3129, 2013.
16. Yoshida S, Arakawa F, Higuchi F, Ishibashi Y, Goto M, Sugita Y, Nomura Y, Niino D, Shimizu K, Aoki R, et al: Gene expression analysis of rheumatoid arthritis synovial lining regions by cDNA microarray combined with laser microdissection: Up-regulation of inflammation-associated STAT1, IRF1, CXCL9, CXCL10, and CCL5. Scand J Rheumatol 41: 170-179, 2012.

17. Saeed AI, Sharov V, White J, Li J, Liang W, Bhagabati N, Braisted J, Klapa M, Currier T, Thiagarajan M, *et al*: TM4: A free, open-source system for microarray data management and analysis. Biotechniques 34: 374-378, 2003.
18. Visone R, Veronese A, Balatti V and Croce CM: MiR-181b: New perspective to evaluate disease progression in chronic lymphocytic leukemia. Oncotarget 3: 195-202, 2012.
19. Tagawa H, Karnan S, Suzuki R, Matsuo K, Zhang X, Ota A, Morishima Y, Nakamura S and Seto M: Genome-wide array-based CGH for mantle cell lymphoma: Identification of homozygous deletions of the proapoptotic gene BIM. Oncogene 24: 1348-1358, 2005.
20. Fernàndez V, Salamero O, Espinet B, Solé F, Royo C, Navarro A, Camacho F, Beà S, Hartmann E, Amador V, *et al*: Genomic and gene expression profiling defines indolent forms of mantle cell lymphoma. Cancer Res 70: 1408-1418, 2010.
21. Simone NL, Soule BP, Ly D, Saleh AD, Savage JE, Degraff W, Cook J, Harris CC, Gius D and Mitchell JB: Ionizing radiation-induced oxidative stress alters miRNA expression. PLoS One 4: e6377, 2009.
22. Ofir M, Hacohen D and Ginsberg D: MiR-15 and miR-16 are direct transcriptional targets of E2F1 that limit E2F-induced proliferation by targeting cyclin E. Mol Cancer Res 9: 440-447, 2011.
23. Rahman M, Lovat F, Romano G, Calore F, Acunzo M, Bell EH and Nana-Sinkam P: miR-15b/16-2 regulates factors that promote p53 phosphorylation and augments the DNA damage response following radiation in the lung. J Biol Chem 289: 26406-26416, 2014.
24. Lu YC, Chen YJ, Wang HM, Tsai CY, Chen WH, Huang YC, Fan KH, Tsai CN, Huang SF, Kang CJ, *et al*: Oncogenic function and early detection potential of miRNA-10b in oral cancer as identified by microRNA profiling. Cancer Prev Res (Phila) 5: 665-674, 2012.
25. Sun G, Shi L, Yan S, Wan Z, Jiang N, Fu L, Li M and Guo J: MiR-15b targets cyclin D1 to regulate proliferation and apoptosis in glioma cells. BioMed Res Int 2014: 687826, 2014.
26. Lovat F, Fassan M, Gasparini P, Rizzotto L, Cascione L, Pizzi M, Vicentini C, Balatti V, Palmieri D, Costinean S, *et al*: miR-15b/16-2 deletion promotes B-cell malignancies. Proc Natl Acad Sci USA 112: 11636-11641, 2015.